PERGAMON

Atmospheric Environment 33 (1999) 3635–3649

ATMOSPHERIC ENVIRONMENT

Studying the effects of calcium and magnesium on size-distributed nitrate and ammonium with EQUISOLV II

Mark Z. Jacobson

Department of Civil and Environmental Engineering, Stanford University, Stanford, CA 94305-4020, USA

Received 6 August 1998; accepted 22 January 1999

Abstract

A chemical equilibrium code was improved and used to show that calcium and magnesium have a large yet different effect on the aerosol size distribution in different regions of Los Angeles. In the code, a new technique of solving individual equilibrium equations was developed. The technique, the analytical equilibrium iteration (AEI) method, gives the same solutions (to at least 7 decimal places) as the previous technique used, the mass-flux iteration (MFI) method, but consumes 13–48 times less computer time. The model was also updated to include treatment of potassium, calcium, magnesium, and carbonate. Previously, it treated only nitrate, ammonium, chloride, sulfate, and sodium. Predictions from the updated code, EQUISOLV II, were compared with data from an eight-stage Berner impactor at Long Beach, Claremont, and Riverside during the Southern California Air Quality Study. When any equilibrium solver is applied between the gas phase and multiple aerosol size bins, unique solutions are possible only when solids (e.g., NH_4NO_3) that form from two gas-phase species are absent. For this study, unique solutions were possible only when the relative humidity exceeded 62%, and only cases in this regime are discussed. Base-case predictions of nitrate and ammonium matched observations well in most size bins of every case. When Ca and Mg were removed from calculations, coarse-mode nitrate decreased at Long Beach, as expected, to maintain charge balance. At Riverside, removing Ca and Mg had the opposite effect, increasing coarse-mode nitrate, shifting it from the accumulation mode. The reason is explained in terms of mean mixed activity coefficients. At Claremont, the charge-balance and activity-coefficient effects nearly canceled each other.

Keywords: Aerosol composition; Aerosol size distribution; Thermodynamic equilibrium; Smog; Numerical methods

1. Introduction

This paper discusses advancements in a chemical equilibrium code and an application of the code to a study of the effects of calcium and magnesium on the size distribution of inorganic particle components. The code used for the study is EQUISOLV II, which is an updated version of EQUISOLV (Jacobson et al., 1996; Jacobson, 1999). The advancements in EQUISOLV II include a new method of solving individual equilibrium equations and an expansion of the code to include the potassium, calcium, magnesium, and carbonate systems. The new numerical method gives the same results as the previous method used, but is 13–48 times faster. Since all equilibrium models are notorious for consuming significant computer time in 3-D models, improving their speed is an important goal. Equilibrium predictions from the revised model are compared with size-distributed measurements from the Southern California Air Quality Study (SCAQS). A sensitivity test is run to estimate the effects of calcium and magnesium on the aerosol size distribution, and a surprising result is found.

Several equilibrium models, listed in Table 1, have been developed to date. Most solve equilibrium problems with either an iterative method that minimizes the Gibbs free energy, an iterative bisection method, or an iterative Newton–Raphson method. Most models have treated the ammonium-nitrate–sulfate system or the ammonium–

1352-2310/99/$ - see front matter
PII: S1352-2310(99)00105-3

Table 1
List of atmospheric equilibrium models, the system they treat, and the numerical method they use to solve equilibrium problems

Model name	Reference	System solved	Solution method
EQUIL	Bassett and Seinfeld (1983)	NH_4–NO_3–SO_4	Iterative Gibbs free energy minimization method
KEQUIL	Bassett and Seinfeld (1984)	NH_4–NO_3–SO_4	Iterative Gibbs free energy minimization method
MARS	Saxena et al. (1986)	NH_4–NO_3–SO_4	Iterative Newton–Raphson method
SEQUILIB	Pilinis and Seinfeld (1987)	NH_4–Na–NO_3–SO_4–Cl	Iterative bisection method
AIM	Wexler and Seinfeld (1991)	NH_4–Na–NO_3–SO_4–Cl	Iterative Gibbs free energy minimization method
SCAPE	Kim et al. (1993a,b)	NH_4–Na–NO_3–SO_4–Cl	Iterative bisection + bisection–Newton for H^+
SCAPE2	Kim and Seinfeld (1995) Meng et al. (1995)	NH_4–Na–Ca–Mg–K–NO_3 –SO_4–Cl–CO_3	Iterative bisection method
MARS-A	Binkowski and Shankar (1995)	NH_4–NO_3–SO_4	Iterative Newton–Raphson method
EQUISOLV	Jacobson et al. (1996)	NH_4–Na–NO_3–SO_4–Cl	Mass-flux iteration method
ISORROPRIA	Nenes et al. (1999)	NH_4–Na–NO_3–SO_4–Cl	Iterative bisection + bisection–Newton for H^+
GFEMN	Ansari and Pandis (1999)	NH_4–Na–NO_3–SO_4–Cl	Iterative Gibbs free energy minimization method
AIM2	Clegg et al. (1998)	NH_4–Na–NO_3–SO_4–Cl	Iterative Gibbs free energy minimization method
EQUISOLV II	This work	NH_4–Na–Ca–Mg–K–NO_3 –SO_4–Cl–CO_3	Analytical equilibrium iteration + mass-flux iteration

sodium–nitrate–chloride–sulfate system. To date, SCAPE2 has treated potassium, calcium, magnesium, and carbonate as well.

An intercomparison of SCAPE2, AIM2, and EQUISOLV II with respect to the ammonium–sodium–nitrate–sulfate–chloride system was performed by Zhang et al. (1999). Two-hundred comparisons for relative humidities (RHs) of 10–95%, HNO_3 of 4.29–38.6 μg m^{-3}, NH_3 of 1.73–13.88 μg m^{-3}, and NaCl of 0–23.8 μg m^{-3} were carried out at a constant temperature of $T = 298.15$ K and particulate H_2SO_4 concentration of 20 μg m^{-3}. Gases were assumed to equilibrate with particulate solids, solution-phase liquids, and solution-phase ions. When similar equilibrium equations were solved, total particulate matter predictions, averaged over all 30% RH cases (20 total), varied between EQUISOLV II and AIM2 by 3%, between EQUISOLV II and SCAPE2 by 6%, and between AIM2 and SCAPE2 by 8%. All three models predicted similar results in general, although some differences arose in certain concentration and relative humidity (RH) regimes. Zhang et al. (1999) describe similarities and differences among the equilibrium models tested.

EQUISOLV II can be applied in two ways. First, it can be used to solve equilibrium equations between the gas phase and multiple size bins of the aerosol (or cloud drop) phase. In such cases, diffusion-limited mass transfer between the gas and particle phases is ignored. Second, it can be used to solve internal aerosol equilibrium to provide saturation vapor pressure terms for diffusion-limited mass transfer equations between the gas and multiple-bin aerosol phases. In Jacobson (1997,1999), a method of coupling saturation vapor pressure terms from equilibrium calculations with nonequilibrium gas–aerosol transfer equations was given.

2. Updated thermodynamic data

EQUISOLV II solves sets of equilibrium equations, each of the form, $v_D D + v_E E + \cdots \rightleftharpoons + v_A A + v_B B + \cdots$, where A, B, C, and D are gases, dissolved liquids, dissolved ions, or solids, and the v's are dimensionless stoichiometric coefficients. The equilibrium-coefficient relation arising from this equation is

$$\frac{\{A\}^{v_A}\{B\}^{v_B}\cdots}{\{D\}^{v_D}\{E\}^{v_E}\cdots} = K_{eq}(T), \tag{1}$$

where $K_{eq}(T)$ is the temperature-dependent equilibrium coefficient and $\{X\}$ is the thermodynamic activity of species X. Appendix Table B.7 of Jacobson (1999) lists many of the equilibrium reactions and temperature-dependent equilibrium-coefficient parameters available in EQUISOLV II.

Equilibrium-coefficient expressions, such as Eq. (1), require mean mixed activity coefficients. The expression

for $NH_3(g) + HNO_3(g) \rightleftharpoons NH_4^+ + NO_3^-$ is

$$\frac{\{NH_4^+\}\{NO_3^-\}}{\{NH_3(g)\}\{HNO_3(g)\}} = \frac{\mathbf{m}_{NH_4^+}\mathbf{m}_{NO_3^-}\gamma^2_{NH_4^+,NO_3^-}}{p_{NH_3}(g)p_{HNO_3}(g)} = K_{eq}(T) \quad (\text{mol}^2\,\text{kg}^{-2}\,\text{atm}^{-2}), \quad (2)$$

where the **m**'s are molalities (mol kg^{-1}), the p's are gas-phase partial pressures (atm), and $\gamma_{NH_4^+,NO_3^-}$ is the mean mixed activity coefficient of NH_4NO_3. In EQUISOLV II, mean mixed activity coefficients are calculated with the empirical mixing rule of Bromley (1973), as described in Jacobson (1999). This method requires mean binary activity coefficients. Jacobson et al. (1996) gave temperature-dependent coefficients for several electrolytes. Here, binary activity coefficient polynomial expressions of the form

$$\ln \gamma^0_{12b} = B_0 + B_1\mathbf{m}_{12}^{1/2} + B_2\mathbf{m}_{12} + B_3\mathbf{m}_{12}^{3/2} + \cdots \quad (3)$$

were obtained for several electrolytes containing potassium, calcium, magnesium, and carbonate. B_0, B_1, ... are fitting coefficients for each electrolyte, given in Table 2.

The liquid water content in EQUISOLV II is determined with the Zdanovskii–Stokes–Robinson (ZSR) method (Stokes and Robinson, 1966). The form of the equation used is

$$c_w = \frac{1000}{m_v}\sum_{i=1}^{N_C}\left(\sum_{j=1}^{N_A}\frac{c_{i,j,m}}{\mathbf{m}_{i,j,a}}\right), \quad (4)$$

where N_C and N_A are the number of cations and anions, respectively, in solution, c_w is the liquid-water content in a size bin in units of mole concentration (moles of liquid water per cubic centimeter of air), m_v is the molecular weight of water (18.02 g mol^{-1}), 1000 converts grams to kilograms, $c_{i,j,m} = \mathbf{m}_{i,j,a}c_w m_v/1000$ is the number of moles of electrolyte pair i, j per cubic centimeter of air in a solution containing all solutes at the ambient RH, and $\mathbf{m}_{i,j,a}$ is the molality of the electrolyte pair alone in solution at the ambient RH. Experimental data for water activity as a function of binary electrolyte molality have been widely measured (e.g., Robinson and Stokes, 1955; Pitzer and Mayorga, 1973; Cohen et al., 1987a,1987b; Tang and Munkelwitz, 1994; Tang, 1997). For several electrolytes, such data were fitted to polynomials of the form

$$\mathbf{m}_{i,j,a} = Y_{0,i,j} + Y_{1,i,j}a_w + Y_{2,i,j}a_w^2 + Y_{3,i,j}a_w^3 + \cdots, \quad (5)$$

where the Y's are polynomial coefficients. Appendix Table B.10 of Jacobson (1999) lists Y's for the electrolytes HCl, HNO_3, H + /HSO_4^-, 2H + /SO_4^{2-}, NaCl, $NaNO_3$, $NaHSO_4$, Na_2SO_4, NH_4Cl, NH_4NO_3, NH_4HSO_4, and $(NH_4)_2SO_4$. Table 9 of Kim and Seinfeld (1995) and Table 8 of Meng et al. (1995) give Y's for KCl, K_2SO_4, KNO_3, $CaCl_2$, $Ca(NO_3)_2$, $MgCl_2$, $MgSO_4$, Na_2CO_3, $NaHCO_3$, K_2CO_3, $KHCO_3$, $Ca(HCO_3)_2$, $Mg(HCO_3)_2$, and NH_4HCO_3 as well. The coefficients for $Ca(NO_3)_2$ and $MgSO_4$, given by Kim and Seinfeld, appear to contain a typographical error. Coefficients used here were obtained by fitting Eq. (5) to their Figs. 15 and 17, respectively.

Solids in EQUISOLV II can form under one of two conditions. If the RH is increasing, the solid phase of an electrolyte is permitted (but not required) to form if the RH is below its deliquescence relative humidity (DRH). The solid phase of an electrolyte is not permitted to form when the RH exceeds the electrolyte's DRH, even if the electrolyte is in a multicomponent mixture. If the RH is decreasing and decreases below the DRH, solutions are assumed to remain supersaturated (in metastable equilibrium) until the crystallization relative humidity (CRH) is reached. The CRH is always less than or equal to the DRH. Some electrolytes, such as NH_3, HNO_3, HCl, and H_2SO_4 do not have a solid phase at room temperature and, therefore, do not have a DRH or a CRH at this temperature. Table 18.4 of Jacobson (1999) lists the DRHs and CRHs of several electrolytes used in EQUISOLV II. SCAPE2, AIM2, and GFEMN also treat crystallization and deliquescence.

3. Overview of the solution techniques used in EQUISOLV II

Atmospheric equilibrium problems can be described with a set of equilibrium equations, activity-coefficient equations, a water-content equation, mass-balance equations, and charge-balance equations. Suppose H^+, NO_3^-, and liquid water, each in two aerosol size bins, and $HNO_3(g)$ are considered. The unique solution to these seven unknown concentrations at equilibrium can be obtained from seven equations – one mass balance equations for total nitrate, one charge balance equations in each bin, one equilibrium/activity-coefficient equation for the reaction $HNO_3(g) \rightleftharpoons H^+ + NO_3^-$ in each bin, and one water equations in each bin. One way to solve this set of algebraic equations is with a nonlinear equation solver. Most such solvers require a first guess and have potential to converge to incorrect, negative roots when the number of equations becomes large. If incorrect convergence occurs, a new guess is required, increasing computer time.

EQUISOLV II iteratively solves the same set of equations as described above, but is positive-definite, mass-conserving, and charge-conserving at any point along the iteration sequence. When a unique, positive solution exists to a set of x unique equilibrium-related equations and x unknowns, EQUISOLV II converges when sufficient iterations are taken. Since it is positive-definite, the solution it converges to in each case must be the unique solution. For some cases, no unique solution exists.

Table 2
Parameters, which fit into Eq. (3), for calculating electrolyte mean binary activity coefficients at 298.15 K

Parameter	$A_{NH_4HCO_3}$ 40 m	B_{NaHCO_3} 6 m	$B_{Na_2CO_3}$ 3.2 m	C_{KNO_3} 9 m
B_0	$-4.7670563231\times10^{-3}$	$-9.1797284136\times10^{-4}$	$-1.2733530328\times10^{-2}$	$-4.5378426057\times10^{-4}$
B_1	$-1.0755382636\times10^{0}$	$-1.1450639746\times10^{0}$	$-3.5606427513\times10^{0}$	$-1.1570027902\times10^{0}$
B_2	$5.7126101252\times10^{-1}$	$8.8699190674\times10^{-1}$	5.3327940147×10^{0}	$7.4160561599\times10^{-1}$
B_3	$-3.1192767536\times10^{-1}$	$-5.4627647371\times10^{-1}$	$-6.0333945024\times10^{0}$	$-6.7300137209\times10^{-1}$
B_4	9.489838942×10^{-2}	$2.4279128196\times10^{-1}$	4.0578729673×10^{0}	$3.5767019273\times10^{-1}$
B_5	$-1.6914582348\times10^{-2}$	$-6.5650768456\times10^{-2}$	$-1.5178863941\times10^{0}$	$-1.1108888851\times10^{-1}$
B_6	$1.6092822753\times10^{-3}$	$9.6885024591\times10^{-3}$	$2.9714499353\times10^{-1}$	$1.9570990945\times10^{-2}$
B_7	$-6.2991860432\times10^{-5}$	$-5.9652548181\times10^{-4}$	$-2.3651713729\times10^{-2}$	$-1.4487200636\times10^{-3}$
	C_{KCl} 30 m	D_{KHSO_4} 6 m	$C_{K_2SO_4}$ 6 m	B_{KHCO_3} 6 m
B_0	$-5.0828419702\times10^{-3}$	$-2.1578619478\times10^{-4}$	$-1.3237616784\times10^{-2}$	$-3.5398320142\times10^{-4}$
B_1	$-1.0569653051\times10^{0}$	$-1.1641075396\times10^{0}$	$-3.5918579554\times10^{0}$	$-1.1606734777\times10^{0}$
B_2	$9.0561950265\times10^{-1}$	1.1887780893×10^{0}	4.2814751245×10^{0}	$8.6435877322\times10^{-1}$
B_3	$-5.0247715978\times10^{-1}$	$-1.1442441446\times10^{0}$	$-3.8523004505\times10^{0}$	$-5.3357720561\times10^{-1}$
B_4	$1.8666053852\times10^{-1}$	$7.3239960308\times10^{-1}$	2.1825294216×10^{0}	$2.4718464783\times10^{-1}$
B_5	$-3.9981652491\times10^{-2}$	$-2.8741101937\times10^{-1}$	$-7.0771656856\times10^{-1}$	$-8.0653609832\times10^{-2}$
B_6	$4.4722941689\times10^{-3}$	$6.2591661774\times10^{-2}$	$1.2087380573\times10^{-1}$	$1.4082858352\times10^{-2}$
B_7	$-2.0420309281\times10^{-4}$	$-5.7777384874\times10^{-3}$	$-8.4282926089\times10^{-3}$	$-1.0409904214\times10^{-3}$
	$B_{K_2CO_3}$ 6 m	$C_{Ca(NO_3)_2}$ 4 m	C_{CaCl_2} 8 m	$C_{CaSO_4\cdot2H_2O}$ 6 m
B_0	$-1.88704\,46206\times10^{-2}$	$-5.4753516204\times10^{-3}$	$-1.1957370489\times10^{-2}$	$2.4702822028\times10^{-4}$
B_1	$-3.3931183411\times10^{0}$	$-3.7960367616\times10^{0}$	$-3.5709097731\times10^{0}$	$-1.0815393680\times10^{1}$
B_2	4.8638449561×10^{0}	7.2643747682×10^{0}	6.6072384297×10^{0}	2.2071007156×10^{1}
B_3	$-4.6172237227\times10^{0}$	$-9.3918454214\times10^{0}$	$-7.1646960564\times10^{0}$	$-2.9921112310\times10^{1}$
B_4	2.7673244331×10^{0}	7.6355127551×10^{0}	5.0843166807×10^{0}	2.4070560375×10^{1}
B_5	$-9.2807321462\times10^{-1}$	$-3.5639838096\times10^{0}$	$-2.0089869519\times10^{0}$	$-1.1055862687\times10^{1}$
B_6	$1.6160131981\times10^{-1}$	$8.7000066239\times10^{-1}$	$4.1350066728\times10^{-1}$	2.6922732476×10^{0}
B_7	$-1.1409384866\times10^{-2}$	$-8.7018844194\times10^{-2}$	$-3.4599185852\times10^{-2}$	$-2.6951199545\times10^{-1}$
	$C_{Mg(NO_3)_2}$ 6 m	C_{MgCl_2} 13 m	C_{MgSO_4} 10 m	
B_0	$-5.9072741959\times10^{-3}$	$-2.1046221178\times10^{-2}$	$-2.4906154237\times10^{-2}$	
B_1	$-3.7752574274\times10^{0}$	$-3.3163138235\times10^{0}$	$-9.4657119484\times10^{0}$	
B_2	7.9541931276×10^{0}	5.5300201794×10^{0}	1.6919611097×10^{1}	
B_3	$-9.9983696576\times10^{0}$	$-4.9131637773\times10^{0}$	$-1.9094948422\times10^{1}$	
B_4	8.2053648546×10^{0}	3.0142160854×10^{0}	1.2561289606×10^{1}	
B_5	$-3.8442136324\times10^{0}$	$-1.0133865621\times10^{0}$	$-4.6049414510\times10^{0}$	
B_6	$9.4031457817\times10^{-1}$	$1.7737598817\times10^{-1}$	$8.8774465027\times10^{-1}$	
B_7	$-9.4155187822\times10^{-2}$	$-1.2564521840\times10^{-2}$	$-6.9870316879\times10^{-2}$	

The coefficients were derived from Pitzer parameters given in A, Roy et al. (1983); B, Harvie et al. (1984); C, Pitzer (1979); D, Clegg and Brimblecombe (1988). Molalities are the maximum molalities for which the fits are valid.

Specifically, when the reactions

$$NH_4NO_3(s) \rightleftharpoons NH_3(g) + HNO_3(g) \quad (6)$$

$$NH_4Cl(s) \rightleftharpoons NH_3(g) + HCl(g) \quad (7)$$

are solved among multiple size bins, and if one of the solids forms, the distribution of the solid among size bins cannot be uniquely determined (Wexler and Seinfeld, 1990), but the partial pressures of the gases can be uniquely determined. The total ammonium, nitrate, and chloride in the system is conserved during the calculation, but no equation ties the mass of the solids to any particular size bin. When these reactions are solved over one size bin, a unique numerical solution does exist.

Similarly, when NH_4NO_3(s) or NH_4Cl(s) precipitate from ions in multiple size bins, and the ions are in

equilibrium with the gas phase, no unique numerical solution to the solid concentrations exist, but unique solutions to the ion concentrations in each bin and to the gas-phase partial pressures exist. When solids containing sulfate, sodium, calcium, magnesium, or potassium, are considered over multiple bins, unique solutions exist. Since sulfate, sodium, etc., are involatile, solids containing them cannot transfer among bins through the gas phase, and unique solutions can be found.

In sum, equilibrium simulations of the direct or indirect formation of NH_4NO_3(s) or NH_4Cl(s) over multiple size bins result in relatively arbitrary distributions of these solids among the bins, regardless of the algorithm used. Unique solutions to problems involving the formation of NH_4NO_3(s) and NH_4Cl(s) over multiple bins can be obtained if diffusion-limited growth equations are solved between the gas phase and each particle size bin, and equilibrium equations are solved within each bin.

EQUISOLV II solves a set of equilibrium equation by solving one equation at a time and repeating the sequence over all equation, many times. Since the solution to each equation requires the transfer of mass and charge from one side of an equilibrium equation to the other, mass and charge are conserved during the iteration sequence so long as individual reactions are mass- and charge-conserving and the system starts in charge balance (thus, separate charge and mass balance equations are not necessary to solve). The reaction $HNO_3(g) = H^+ + NO_3^-$ conserves mass and charge. The charge balance constraint allows initial charges to be distributed among all dissociated ions, but the initial sum, over all species of charge multiplied by molality must equal zero. The simplest way to initialize charge is to set all ion molalities to zero. Initial mass in the system can be distributed arbitrarily, subject to the charge balance constraint.

Suppose solutions to several unique equilibrium equations within each size bin and between each size bin and the gas phase are required. The original EQUISOLV code required three types of iteration procedures. Individual equilibrium equations were first iterated (level-3 iteration). When one equation converged, the updated concentrations were used as inputs into subsequent equations. The sequence over all equations was repeated several times (level-2 iteration), but in reverse order every other time, until the normalized difference in species concentrations from sequence to sequence fell below a specified "local" error tolerance. During level-2 and -3 iterations, water contents and activity coefficients were held fixed. Only when the local convergence criterion was met were the activity coefficients and water contents updated. At that point, the level-2 and -3 iterations were repeated several times (level-1 iteration). When the normalized difference in concentrations between sequential local error tolerance checks fell below a specified "global" error tolerance, the system was said to have converged. The global and local error tolerances can be set strict enough to ensure convergence when a unique solution exists.

In EQUISOLV, the mass flux iteration (MFI) method was used to iterate each equilibrium equation (level-3 iterations). The advantage of this method was that it converged all types of individual equilibrium equations, including complex equations, it solved equations to high precision, even when concentration differences in an equation were much larger than the roundoff error of the machine, and it required no intelligent first guess. The disadvantage were that it required up to 50 or more iterations to converge many equations under typical conditions. Here, a method of replacing the MFI method for nearly all types of equilibrium reactions is discussed. Although two new techniques are actually described, each applicable to different types of equilibrium reactions, each technique is referred to as an analytical equilibrium iteration (AEI) method, for simplicity.

The first AEI method discussed replaces the MFI solution method for reactions of the form, $D \rightleftharpoons A$, $D \rightleftharpoons A + B$, and $D + E \rightleftharpoons A + B$. Reactions of this type make up over 80% of the equations in Appendix Table B. 7 of Jacobson (1999). The method requires solving each equilibrium equation analytically instead of with a level-3 iteration when water content and activity coefficients are held constant. This method was described for reactions of the form $D \rightleftharpoons A$ in Jacobson et al. (1996, p. 9087). Here, analytical solutions for equations aside from those of the form $D \rightleftharpoons A$ are introduced. A technique of eliminating roundoff error in the analytical solution is also given. This technique is needed only to ensure high precision. Whereas roundoff errors affect species with low concentrations by 1–50 or more orders of magnitude, reducing roundoff error for an individual reaction is usually not necessary, since total mass in the system is hardly affected. The accumulated error in time and space due to neglecting the roundoff error correction has been found to be about 1% of total mass after 3 days of simulation over a 3-D grid. Another method of reducing error is to double the precision of the computer, say from 14–16 digits to 28–32 digits. Many computers cannot achieve such accuracy. Other computers, such as a Cray, require a fourfold increase in computer time with a doubling of precision to 28 digits. Adding one predictor step to reduce roundoff error accomplishes the same result as doubling precision to 28–32 digits, but with the use of less than one-fourth the additional computer time. Adding two predictor steps is equivalent to 42–48 digits of precision.

Reactions of the form $D \rightleftharpoons 2A + B$ and $D \rightleftharpoons A + 2B$ make all but one of the remaining reactions in Appendix Table B.7 of Jacobson (1999). Because these equations give rise to third-order polynomials, they cannot be solved analytically with the first AEI method. Instead, they must be solved iteratively with another method. An

iterative AEI method of solving these equations that nearly eliminates roundoff error is discussed. This method requires, on average, half as many iterations as the MFI method.

In sum, two AEI methods are discussed. One solves reactions of the form $D \rightleftharpoons A$, $D \rightleftharpoons A + B$, and $D + E \rightleftharpoons A + B$ and the other solves reactions of the form $D \rightleftharpoons 2A + B$ and $D \rightleftharpoons A + 2B$. The only other type of reaction in Appendix Table B. 7 of Jacobson (1999) has the form $D \rightleftharpoons 3A + B + C$. Because of its complexity, this type of reaction is still solved with the MFI method.

4. AEI solutions for individual reactions

In this section, the AEI method is described for different types of equilibrium equations. In all cases, solutions are obtained by first converting gas and aerosol concentrations in equilibrium-coefficient expressions to mole concentrations with $c_g = p_g/R^*T$ and $c_a = \mathbf{m}_a c_w m_v/1000$, where c, p, and $\mathbf{m}$ are the mole concentration (moles per cubic centimeter of air), partial pressure (atm), and molality (moles per kilogram of water) of a gas (g) or aerosol component (a), R^* is the universal gas constant (82.06 cm^3 atm mol^{-1} K^{-1}), T is temperature (K), and 1000 converts g to kg. Once partial pressures and molalities have been converted to mole concentrations, all other terms in an equilibrium coefficient expression [R^*, T, c_w, m_v, water activity (a_w), and activity coefficients (γ)], which are assumed to be known inside level-2 iterations, are moved to the same side of the equation as the equilibrium coefficient (Table 3). The mole concentrations are then solved for, as described below.

4.1. Reactions of the form $D \rightleftharpoons A$

Solutions to reactions of the form $D \rightleftharpoons A$ are assumed not to result in significant roundoff error, since they do not involve the use of the quadratic equation. Table 3 identifies reaction types of this form and their modified equilibrium-coefficient expressions. The analytical solution to the modified expression is found from

$$\frac{c_{A,c}}{c_{D,c}} = \frac{c_{A,0} + \Delta x_{fin}}{c_{D,0} - \Delta x_{fin}} = K_r \tag{8}$$

where the subscript 0 indicates an initial value, the subscript c indicates a converged value, Δx_{fin} is the change in mole concentration required to converge the solution from its initial values, and $c_{A,c} = c_{A,0} + \Delta x_{fin}$; $c_{D,c} = c_{D,0} - \Delta x_{fin}$. Since Δx_{fin} is the same for each species in the equation, the solution to this equation,

$$\Delta x_{fin} = \frac{c_{D,0} - c_{A,0} K_r}{1 + K_r} \tag{9}$$

is mass and charge conserving.

4.2. Nonprecipitation reactions of the form $D + E \rightleftharpoons A + B$

Nonprecipitation reactions of the form $D + E \rightleftharpoons A + B$, identified in Table 3, are solved analytically, but with the option of one or more predictor steps to reduce roundoff error. Table 3 identifies reactions of this form. The analytical solution is found by solving

$$\frac{c_{A,c} c_{B,c}}{c_{D,c} c_{E,c}} = \frac{(c_{A,1} + \Delta x_{fin})(c_{B,1} + \Delta x_{fin})}{(c_{D,1} + \Delta x_{fin})(c_{E,1} + \Delta x_{fin})} = K_r \tag{10}$$

where $c_{A,1}$, $c_{B,1}$, $c_{D,1}$, and $c_{E,1}$ are initial mole concentrations if no predictor step is taken or estimated concentrations if one is taken, and

$$\begin{aligned} c_{A,c} &= c_{A,1} + \Delta x_{fin}, \quad c_{B,c} = c_{B,1} + \Delta x_{fin}, \\ c_{D,c} &= c_{D,1} + \Delta x_{fin}, \quad c_{E,c} = c_{E,1} + \Delta x_{fin}. \end{aligned} \tag{11}$$

are converged final concentrations of each species. The solution to Eq. (10) is

$$\Delta x_{fin} = \frac{-c_{A,1} - c_{B,1} - c_{D,1} K_r - c_{E,1} K_r + \sqrt{(c_{A,1} + c_{B,1} + c_{D,1} K_r + c_{E,1} K_r)^2 - 4(1 - K_r)(c_{A,1} c_{B,1} - c_{D,1} c_{E,1} K_r)}}{2(1 - K_r)} \tag{12}$$

In many cases, assuming $c_{A,1}, \ldots, c_{E,1}$ are initial values and substituting Eq. (12) into Eq. (10) gives an exact solution to (10). When differences in concentration or in products of concentrations are greater than the precision of the computer, roundoff error arises in Eq. (12). Also, when Δx_{fin} is applied to Eq. (11), a roundoff error arises if the difference between Δx_{fin} and the initial concentration is smaller than the computer precision.

Suppose two gases, NH_3(g) and HNO_3(g) equilibrate with two ions, NH_4^+ and NO_3^- by the reaction $NH_3(g) + HNO_3(g) \rightleftharpoons NH_4^+ + NO_3^-$ in a single aerosol size bin. For a liquid water content of 1 μg m^{-3} (5.88×10^{-14} mol cm^{-3}), $K_r = 1.5 \times 10^{-4}$ at 298.15 K. Suppose the initial concentrations of NH_3(g), HNO_3(g), NH_4^+, and NO_3^- before the equation is solved are 2.4×10^{-12} μg m^{-3} (1.4×10^{-25} mol cm^{-3}), 8.8×10^{-12} μg m^{-3} (1.4×10^{-25} mol cm^{-3}), 2.5×10^{-12} μg m^{-3} (1.4×10^{-25} mol cm^{-3}), and 0.87 μg m^{-3} (1.4×10^{-14} mol cm^{-3}), respectively. All initial concentrations, except that of NH_4^+(g), are small. Substituting Eq. (12) into Eq. (10) on a computer with 16 digits of accuracy gives $F_{AE1(0)} = K_r c_{D,c} c_{E,c}/c_{A,c} c_{B,c} = 2.3 \times 10^{-9}$, indicating that

Table 3
Types of reactions solved with the AEI method, corresponding equilibrium coefficient equations, corresponding equilibrium coefficient equations that are solved, and corresponding modified equilibrium coefficients

Reaction	Equilibrium coefficient expression	Modified expression	Modified equilibrium coefficient
Reactions of the form $D \rightleftharpoons A$			
$D(g) \rightleftharpoons A(aq)$	$\frac{\mathbf{m}_A}{p_D} = K_{eq}$	$\frac{c_A}{c_D} = K_r$	$K_r = K_{eq}\left(\frac{c_w m_v}{1000}\right)R^*T$
$D(aq) + H_2O(aq) \rightleftharpoons A(aq)$	$\frac{\mathbf{m}_A}{\mathbf{m}_D a_w} = K_{eq}$	$\frac{c_A}{c_D} = K_r$	$K_r = K_{eq}a_w$
Reactions of the form $D + E \rightleftharpoons A + B$			
$D(g) + E(g) \rightleftharpoons A(aq) + B(aq)$	$\frac{\mathbf{m}_A\mathbf{m}_B}{p_D p_E} = K_{eq}$	$\frac{c_A c_B}{c_D c_E} = K_r$	$K_r = K_{eq}\left(\frac{c_w m_v}{1000}R^*T\right)^2$
$D(g) + E(g) \rightleftharpoons A^+ + B^-$	$\frac{\mathbf{m}_A\mathbf{m}_B\gamma_{AB}^2}{p_D p_E} = K_{eq}$	$\frac{c_A c_B}{c_D c_E} = K_r$	$K_r = K_{eq}\frac{1}{\gamma_{AB}^2}\left(\frac{c_w m_v}{1000}R^*T\right)^2$
$D(aq) + E(aq) \rightleftharpoons A^+ + B^-$	$\frac{\mathbf{m}_A\mathbf{m}_B\gamma_{AB}^2}{\mathbf{m}_D\mathbf{m}_E} = K_{eq}$	$\frac{c_A c_B}{c_D c_E} = K_r$	$K_r = K_{eq}\frac{1}{\gamma_{AB}^2}$
Reactions of the form $D(\neq s) \rightleftharpoons A + B$			
$D(g) \rightleftharpoons A(aq) + B(aq)$	$\frac{\mathbf{m}_A\mathbf{m}_B}{p_D} = K_{eq}$	$\frac{c_A c_B}{c_D} = K_r$	$K_r = K_{eq}\left(\frac{c_w m_v}{1000^2}\right)R^*T$
$D(g) \rightleftharpoons A^+ + B^-$	$\frac{\mathbf{m}_A\mathbf{m}_B\gamma_{AB}^2}{p_D} = K_{eq}$	$\frac{c_A c_B}{c_D} = K_r$	$K_r = K_{eq}\frac{1}{\gamma_{AB}^2}\left(\frac{c_w m_v}{1000}\right)^2 R^*T$
$D(aq) \rightleftharpoons A^+ + B^-$	$\frac{\mathbf{m}_A\mathbf{m}_B\gamma_{AB}^2}{\mathbf{m}_D} = K_{eq}$	$\frac{c_A c_B}{c_D} = K_r$	$K_r = K_{eq}\frac{1}{\gamma_{AB}^2}\left(\frac{c_w m_v}{1000}\right)$
$D^- \rightleftharpoons A^+ + B^{2-}$	$\frac{\mathbf{m}_A\mathbf{m}_B\gamma_{AB}^3}{\mathbf{m}_D\gamma_{AD}^2} = K_{eq}$	$\frac{c_A c_B}{c_D} = K_r$	$K_r = K_{eq}\frac{\gamma_{AD}^2}{\gamma_{AB}^3}\left(\frac{c_w m_v}{1000}\right)$
$D(aq) + H_2O(aq) \rightleftharpoons A^+ + B^-$	$\frac{\mathbf{m}_A\mathbf{m}_B\gamma_{AB}^2}{\mathbf{m}_D a_w} = K_{eq}$	$\frac{c_A c_B}{c_D} = K_r$	$K_r = K_{eq}\frac{a_w}{\gamma_{AB}^2}\left(\frac{c_w m_v}{1000}\right)$
$D^+ \rightleftharpoons A^+ + B(g)$	$\frac{\mathbf{m}_A\gamma_{AF}^2 p_B}{\mathbf{m}_D\gamma_{DF}^2} = K_{eq}$	$\frac{c_A c_B}{c_D} = K_r$	$K_r = K_{eq}\frac{\gamma_{DF}^2}{\gamma_{AF}^2}\frac{1}{R^*T}$
Reactions of the form $D(s) \rightleftharpoons A + B$			
$D(s) \rightleftharpoons A^+ + B^{2-}$	$\mathbf{m}_A\mathbf{m}_B\gamma_{AB}^2 = K_{eq}$	$c_A c_B = K_r$	$K_r = K_{eq}\frac{1}{\gamma_{AB}^2}\left(\frac{c_w m_v}{1000}\right)^2$
$D(s) \rightleftharpoons A^{2+} + B^{2-}$	$\mathbf{m}_A\mathbf{m}_B\gamma_{AB}^2 = K_{eq}$	$c_A c_B = K_r$	$K_r = K_{eq}\frac{1}{\gamma_{AB}^2}\left(\frac{c_w m_v}{1000}\right)^2$
$D(s) \rightleftharpoons A(aq) + B(aq)$	$\mathbf{m}_A\mathbf{m}_B = K_{eq}$	$c_A c_B = K_r$	$K_r = K_{eq}(c_w m_v/1000)^2$
$D(s) \rightleftharpoons A(g) + B(g)$	$p_A p_B = K_{eq}$	$c_A c_B = K_r$	$K_r = K_{eq}\left(\frac{1}{R^*T}\right)^2$
Reactions of the form $D(s) \rightleftharpoons 2A + B$ *and* $D(s) \rightleftharpoons A + 2B$			
$D(s) \rightleftharpoons 2A^+ + B^{2-}$	$\mathbf{m}_A^2\mathbf{m}_B\gamma_{AB}^3 = K_{eq}$	$c_A^2 c_B = K_r$	$K_r = K_{eq}\frac{1}{\gamma_{AB}^3}\left(\frac{c_w m_v}{1000}\right)^3$
$D(s) \rightleftharpoons A^{2+} + 2B^-$	$\mathbf{m}_A\mathbf{m}_B^2\gamma_{AB}^3 = K_{eq}$	$c_A c_B^2 = K_r$	$K_r = K_{eq}\frac{1}{\gamma_{AB}^3}\left(\frac{c_w m_v}{1000}\right)^3$

the analytical solution failed due to roundoff error. For the equation to converge, $F_{AE1(0)}$ must equal unity. The converged solution to this problem is $NH_3(g) = 2.8\times10^{-25}$, $HNO_3(g) = 2.8\times10^{-25}$, $NH_4^+ = 8.4\times10^{-40}$, and $NO_3^- = 1.4\times10^{-14}$ mol cm^{-3}. The computer correctly predicted three of the concentrations but predicted $NH_4^+ = 3.7\times10^{-31}$ mol cm^{-3} (9 orders of magnitude error) causing the error in $F_{AE1(0)}$. While the net error in mass was relatively trivial, a method of reducing roundoff error may be desired.

A method of reducing the magnitude of Δx relative to initial values and, hence, roundoff errors arising from Eqs. (11) and (12) is to estimate values of $c_{A,1}, \ldots, c_{E,1}$ that are closer to the solution than are initial values. The estimated concentrations are

$$c_{A,1} = c_{A,0} + \Delta x_{est}, \quad c_{B,1} = c_{B,0} + \Delta x_{est},$$
$$c_{D,1} = c_{D,0} - \Delta x_{est}, \quad c_{E,1} = c_{E,0} - \Delta x_{est}, \tag{13}$$

where $c_{A,0}, \ldots, c_{E,0}$ are initial concentrations and Δx_{est} is the estimated change in concentration, determined by rewriting Eq. (10) as

$$\frac{[\max(c_{A,0}, c_{B,0})][\max(c_{A,0}, c_{B,0}) + \Delta x_{est}]}{[\max(c_{D,0}, c_{E,0})][\max(c_{D,0}, c_{E,0}) - \Delta x_{est}]} = K_r. \tag{14}$$

The idea here is to put the equilibrium equation in a form similar to Eq. (8) so that it can be solved with Eq. (9). By moving the largest concentrations in Eq. (14) to the right side of the equation and calculating Δx_{est} from the smallest concentrations, an estimated change in the smallest concentrations can be resolved. Since Δx_{est} is applied to all concentrations in Eq. (13), mass is conserved during this process. When Eq. (14) is solved, it is necessary to place outer limits on the solution to ensure that the computer does not predict $c_{A,1} = c_{A,0} + \Delta x_{est} = c_{A,0}$ when $|\Delta x_{est}| \ll c_{A,0}$. Solving Eq. (14) and placing outer limits on the result gives

$$\Delta x_{est} = \min\left[\max\left(\frac{\min(c_{D,0}, c_{E,0})K_r \dfrac{\max(c_{D,0}, c_{E,0})}{\max(c_{A,0}, c_{B,0})} - \min(c_{A,0}, c_{B,0})}{1 + K_r \dfrac{\max(c_{D,0}, c_{E,0})}{\max(c_{A,0}, c_{B,0})}}, -\varepsilon c_{A,0}, -\varepsilon c_{B,0}\right), -\varepsilon c_{D,0}, -\varepsilon c_{E,0}\right]. \tag{15}$$

where ε is a constant, no smaller than the smallest difference from unity on the computer being used. A typical value is $\varepsilon = 1.0 - 1.0 \times 10^{-13}$, which works for a Cray machine in single precision (14 digits of accuracy) or an SGI machine in double precision (16 digits). When the limits in Eq. (15) are hit, more than one iteration of Eq. (15) together with Eq. (13) is needed. Since each predictor step cuts across 13 orders of concentration magnitude when $\varepsilon = 1.0 - 1.0 \times 10^{-13}$, very few iterations of the predictor step are ever needed.

Numerous comparisons of the number of predictor iterations required for the AEI method and total iterations required for the MFI method to solve an equation of the form D + E⇌A + B to seven digits of accuracy were carried out. The concentration range for species was 198 orders of magnitude, and the equilibrium coefficient range was 160 orders of magnitude. In all cases, the AEI method required 50–100 times fewer iterations than did the MFI method to obtain the same precision.

4.3. Reactions of the form D(≠ s) ⇌ A + B

Nonpecipitation reactions of the form D(≠ s) ⇌ A + B can also be solved analytically with the option of a predictor step. Table 3 identifies reaction types of this form. Their converged solution is found by solving

$$\frac{c_{A,c}c_{B,c}}{c_{D,c}} = \frac{(c_{A,1} + \Delta x_{fin})(c_{B,1} + \Delta x_{fin})}{c_{D,1} - \Delta x_{fin}} = K_r \tag{16}$$

where $c_{A,c} = c_{A,1} + \Delta x_{fin}$, $c_{B,c} = c_{B,1} + \Delta x_{fin}$, and $c_{D,c} = c_{D,1} - \Delta x_{fin}$,. The solution is

$$\Delta x_{fin} = \frac{-c_{A,1} - c_{B,1} - K_r + \sqrt{(c_{A,1} + c_{B,1} + K_r)^2 - 4(c_{A,1} + c_{B,1} - c_{D,1}K_r)}}{2}. \tag{17}$$

If a predictor step is used,

$$c_{A,1} = c_{A,0} + \Delta x_{est}, \quad c_{B,1} = c_{B,0} + \Delta x_{est},$$
$$c_{D,1} = c_{D,0} - \Delta x_{est}. \tag{18}$$

Otherwise, $c_{A,1}$, $c_{B,1}$ and $c_{D,1}$ are set to initial values. The estimated change in concentration, Δx_{est}, is found by rewriting Eq. (16) in the form of Eq. (8) as

$$\frac{[\max(c_{A,0}, c_{B,0})][\min(c_{A,0}, c_{B,0}) + \Delta x_{est}]}{c_{D,0} - \Delta x_{est}} = K_r. \tag{19}$$

Solving Eq. (19) and placing outer limits on the result gives

$$\Delta x_{est} = \min\left[\max\left(\frac{\dfrac{c_{D,0}K_r}{\max(c_{A,0}, c_{B,0})} - \min(c_{A,0}, c_{B,0})}{1 + \dfrac{k_r}{\max(c_{A,0}, c_{B,0})}}, -\varepsilon c_{A,0}, -\varepsilon c_{B,0}\right), \varepsilon c_{D,0}\right]. \tag{20}$$

Like with Eqs. (15) and (13), Eqs. (20) and (18) may be iterated if the limits in Eq. (20) are reached.

4.4. *Reactions of the form* $D(s) \rightleftharpoons A + B$

Table 3 identifies precipitation reactions of the form, $D(s) \rightleftharpoons A + B$. Precipitation proceeds only when $(c_{A,0} + c_{D,0})(c_{B,0} + c_{D,0}) > K_r$, where $c_{A,0}$, $c_{B,0}$, and $c_{D,0}$ are initial values. If this criterion is not met, the equation can be skipped until $c_{A,0}$, $c_{B,0}$, $c_{D,0}$, or K_r change. If the criterion is met, the solution can be found analytically, but a predictor step may be applied to reduce roundoff error. The analytical solution is found by solving

$$c_{A,c}c_{B,c} = (c_{A,1} + \Delta x_{fin})(c_{B,1} + \Delta x_{fin}) = K_r \tag{21}$$

where $c_{A,c} = c_{A,1} + \Delta x_{fin}$ and $c_{B,c} = c_{B,1} + \Delta x_{fin}$ are the converged concentrations of the reactants, $c_{D,c} = c_{D,1} + \Delta x_{fin}$ is the converged solid concentration, and $c_{A,1}$, $c_{B,1}$ and $c_{D,1}$ are initial concentrations if no predictor step is taken and estimated concentrations if a step is taken. The analytical solution to Eq. (21) is

$$\Delta x_{fin} = \frac{-c_{A,1} - c_{B,1} + \sqrt{(c_{A,1} + c_{B,1})^2 - 4(c_{A,1}c_{B,1} - K_r)}}{2} \tag{22}$$

If a predictor step is taken, $c_{A,1}$, $c_{B,1}$ and $c_{D,1}$ are found from Eq. (18), where Δx_{est} is determined here by rewriting Eq. (21) in the form of Eq. (8) as

$$[\max(c_{A,0}, c_{B,0})][\min(c_{A,0}, c_{B,0}) + \Delta x_{est}] = K_r. \tag{23}$$

Solving Eq. (23) and placing outer limits on the result gives

$$\Delta x_{est} = \min\left[\max\left(\frac{k_r}{\max(c_{A,0}, c_{B,0})} - \min(c_{A,0}, c_{B,0}), -\varepsilon c_{A,0}, -\varepsilon c_{B,0}\right), \varepsilon c_{D,0}\right]. \tag{24}$$

Like with Eqs. (15) and (13), Eqs. (24) and (18) may be iterated if the limits in Eq. (24) are reached.

4.5. *Solid reactions of the form* $D(s) \rightleftharpoons 2A + B$ *and* $D(s) \rightleftharpoons A + 2B$

Reaction types of the form $D(s) \rightleftharpoons 2A + B$ and $D(s) \rightleftharpoons A + 2B$ are listed in Table 3. A solution to the first equation is discussed here. A solution to the second equation requires merely switching A with B in the solution to the first. A solid can form via the first equation only if $(c_{A,0} + 2c_{D,0})^2(c_{B,0} + c_{D,0}) > K_r$. The converged solution to the first equation is

$$c_{A,c}^2 c_{B,c} = (c_{A,0} + 2\Delta x_{fin})^2(c_{B,0} + \Delta x_{fin}) = K_r, \tag{25}$$

where $c_{A,c} = c_{A,0} + 2\Delta x_{fin}$, $c_{B,c} = c_{B,0} + \Delta x_{fin}$, and $c_{D,c} = c_{D,0} - \Delta x_{fin}$. Rewriting Eq. (25) gives

$$\Delta x_{fin}^3 + q\Delta x_{fin}^2 + r\Delta x_{fin} + s, \tag{26}$$

where $q = c_{A,0} + c_{B,0}$, $r = c_{A,0}c_{B,0} + 0.25c_{A,0}^2$, and $s = c_{A,0}^2 c_{B,0} - K_{eq}$. The solution to Eq. (26) must be obtained iteratively. Applying the Newton–Raphson technique to Eq. (26) gives

$$\Delta x_{n+1} = \Delta x_n - \frac{f(x)}{f'(x)} = \frac{2\Delta x_n^3 + q\Delta x_n^2 - s}{3\Delta x_n^2 + 2q\Delta x_n + r}, \tag{27}$$

where $f(x) = \Delta x_n^3 + q\Delta x_n^2 + r\Delta x_n + s$, $f'(x) = 3\Delta x_n^2 + 2q\Delta x_n + r$, n is the iteration number, and the initial value of Δx in Eq. (27) is set to zero for simplicity. Other iterative techniques of solving this equation are fixed-point iteration and the bisection method. The Newton–Raphson technique converges with fewer iterations than the other two methods for third-order polynomials (Kreyszig, 1983, pp. 760–768). The problem with Eq. (27) when used alone is that roundoff error prevents it from converging if large concentration differences occur relative to the equilibrium coefficient. To minimize error and guarantee convergence for any set of concentrations and equilibrium coefficients, the solution was modified in several ways. First, instead of converging Eq. (27) before applying Δx to concentrations, concentrations were updated after each iteration of Δx. Thus, $c_{A,n+1} = c_{A,n} + 2\Delta x_{n+1}$, $c_{B,n+1} = c_{B,n} + \Delta x_{n+1}$, and $c_{D,n+1} = c_{D,n} - \Delta x_{n+1}$. This required updates of q, r, and s at the beginning of each iteration so that $q_n = c_{A,n} + c_{B,n}$, $r_n = c_{A,n}c_{B,n} + 0.25c_{A,n}^2$, and $s_n = c_{A,n}^2 c_{B,n} - K_{eq}$. Third, Δx_n, used on the right-hand side of Eq. (27) during each iteration, was bounded by $\Delta x_n = \min[\max(\Delta x_n, -0.25c_{A,n}, -0.5c_{B,n}), 0.5c_{D,n}]$. Eq. (27), itself, was also bounded with

$$\Delta x_{n+1} = \min\left[\max\left(\frac{2\Delta x_n^3 + q_n\Delta x_n^2 - s_n}{3\Delta_n^2 + 2q_n\Delta x_n + r_n}, -0.5\varepsilon c_{A,n}, -\varepsilon c_{B,n}\right), \varepsilon c_{D,n}\right]. \tag{28}$$

With this technique, equations of the form $D(s) \rightleftharpoons 2A + B$ converged under all, including extremely severe, conditions tested. For typical atmospheric conditions, the equations always converged in less than 30 iterations.

Many comparisons of the number of iterations required for the AEI and MFI methods to solve an equation of the form $D(s) \rightleftharpoons A + 2B$ to seven digits of accuracy under typical and extreme conditions were

carried out. Under all conditions, the AEI method converged equations about twice as fast as did the MFI method. For typical conditions, the AEI method converged in less than 30 iterations. For extreme conditions, in which concentration variations were up to 159 orders of magnitude (solids could not form below concentrations of 10^{-60} mol cm^{-3} for the equilibrium coefficients chosen), the number of iterations required exceeded 30 but were still about half those required for the MFI method.

In sum, the AEI method required 50–100 times fewer iterations than the MFI method to converge reactions of the form $D \rightleftharpoons A$, $D \rightleftharpoons A + B$, and $D + E \rightleftharpoons A + B$ to seven digits of accuracy. The AEI method required 50% fewer iterations than the MFI method to converge reactions of the form $D \rightleftharpoons 2A + B$ and $D \rightleftharpoons A + 2B$.

5. Speed test of the AEI method

Table 4 shows results from a comparison of the overall speed of EQUISOLV II on a single, scalar processor of an SGI Origin 2000 when the AEI (with one predictor step for the first AEI method) and MFI schemes were used. Equilibrium equations were solved for the ammonium–nitrate–sulfate–sodium–chloride–potassium–calcium–magnesium system for a variety of RHs. The local and global error tolerances used were both 10^{-3}. Simulations with the AEI and MFI methods were carried out in 1 grid cell and 490 grid cells. EQUISOLV II was originally designed for vector machines; thus, every inner loop is vectorized around the grid cell dimension. Even on a scalar machine, this type of looping is optimal, as shown in Jacobson (1998) with respect to solutions to chemical ordinary differential equations. Table 4 shows that, on an SGI Origin 200, EQUISOLV II was 13–48 times faster when the AEI method was used than when the MFI method was used. With the AEI method, EQUISOLV II was 3.5–3.8 times faster per cell when 490 cells were solved together than when one cell was solved at a time. On a Cray J-916, the solution in 490 cells is about 30–40 times faster per cell than it is in one cell.

6. Comparison of model predictions with eight-stage impactor data

To test the equilibrium model, predictions were compared with eight-stage Berner impactor measurements from John et al. (1990) during the Southern California Air Quality Study (SCAQS). The 50% cutoff diameters for each stage were 0.075, 0.14, 0.27, 0.52, 1.04, 2.15, 4.35, and 8.2 μm. The measurements discussed were made at 0500–0830 PST and 1300–1630 PST on August 28, 1987 and 0500–0830 PST on August 28, 1987 at Long Beach, Claremont, and Riverside (Rubidoux) and included size-resolved 3.5-h average concentrations of NH_4^+, Na^+, Mg^{2+}, Ca^{2+}, NO_3^-, Cl^-, NO_3^-, and SO_4^{2-}. Ion imbalances in the measurements were rectified here by adding H^+ or CO_3^{2-}. At Long Beach, the observed accumulation mode was dominated by sulfate, whereas the coarse mode was dominated by nitrate. At Riverside and Claremont, the accumulation and coarse modes were dominated by nitrate, followed by ammonium, then

Table 4
Speed of the MFI method compared with that of the AEI method on a single processor of an SGI Origin 2000 for several cases where $T = 298.15$ K but the RH varied. Other conditions were $NH_3 = 1.73$, $HNO_3 = 12.86$, $H_2SO_4 = 20$, $NaCl = 5.96$, $CaCO_3 = 1.0$, $MgCO_3 = 0.5$, and $K_2CO_3 = 0.3$ μg m^{-3}. One predictor step was taken for the first AEI method. Two computer timings are shown for each scheme – the time per grid cell when 1 cell was solved and the time per cell when 490 cells were solved together. The 490-cell speedup factor is the former divided by the latter. The AEI/MFI speedup factor is the time per cell in 490 cells for the MFI method divided by that for the AEI method and indicates that the AEI method was 13–48 times faster than the MFI method in all cases

	MFI method			AEI method			
R.h.	Time/cell 1 cell (s)	Time/cell 490 cells (s)	490-cell Speedup factor	Time/cell 1 cell (s)	Time/cell 490 cells (s)	490-cell Speedup factor	AEI/MFI Speedup factor
10	5.043	1.398	3.61	0.137	0.0595	2.30	23.5
20	8.227	2.329	3.53	0.215	0.098	2.18	23.8
30	3.349	0.947	3.53	0.149	0.0689	2.162	13.7
40	0.632	0.171	3.71	0.018	0.0073	2.46	23.4
50	0.529	0.142	3.73	0.013	0.00398	3.27	35.7
60	0.499	0.133	3.76	0.011	0.00280	3.93	47.5
70	3.107	0.865	3.59	0.073	0.018	3.98	48.1
80	2.522	0.699	3.61	0.063	0.0168	3.73	41.6
90	2.074	0.569	3.64	0.057	0.0157	3.63	36.2
95	1.955	0.529	3.69	0.054	0.0153	3.52	34.6

sulfate. Nitrate, ammonium, calcium, and magnesium concentrations were higher at Riverside than at Claremont or Long Beach. Sulfate concentrations were highest at Long Beach. The SCAQS database also contained gas-phase concentrations of NH_3 and HNO_3, temperatures, and surface pressures at Long Beach, Claremont and Riverside. RH data in the general database were available at Claremont and Riverside, but not at Long Beach; thus, RHs from nearby Hawthorne were assumed for Long Beach. Gas-phase concentrations of HCl were not available.

Equilibrium calculations were carried out by assuming each stage was a size bin and initializing concentrations in each bin with the observed stage values. Calcium and magnesium were measured only in stages 6 and 7 (2.15 and 4.35 μm cutoff diameters, respectively). Since Ca and Mg exist in larger particles as well, values in stage 8 (8.2 μm cutoff diameter) were assumed to equal those in stage 7 in the model. Gas concentrations were initialized with observations.

During the calculations, ammonia–ammonium and nitric acid–nitrate were allowed to transfer between the gas and particle phases. The goal of the tests was to determine whether the model could predict the equilibrium size distributions of ammonium and nitrate. If the model did not work, if data were insufficient or if the system were out of equilibrium, the calculated equilibrium distributions would not match the initial distributions. Since a unique solution exists for each equilibrium problem that consists of x equations and x unknowns, it does not matter whether all the initial particulate ammonium and nitrate are distributed in the particle or gas phase. Indeed, when all measured ammonium and nitrate were initially removed from particles and added to the gas phase, the model predicted the same distributions as when the model was initialized with measured ammonium and nitrate in each size bin. Thus, a unique numerical equilibrium solution existed in each case that consisted of x equations and x unknowns.

All substances, aside from nitrate and ammonium, were constrained to their initial size bin, since most were involatile. Chloride, which is volatile, was constrained to the particle phase, since no gas data were available to initialize it. Within each bin, the modeled species that could possibly form included H_2O(aq), H_2CO_3(aq), H_2SO_4(aq), H^+, NH_4^+, Na^+, Mg^{2+}, Ca^{2+}, K^+, NO_3^-, Cl^-, HSO_4^-, SO_4^{2-}, HCO_3^-, CO_3^{2-}, NH_4NO_3(s), NH_4Cl(s), NH_4HSO_4(s), $(NH_4)_2SO_4$(s), $(NH_4)_3H(SO_4)_2$(s), NH_4HCO_3(s), $NaNO_3$(s), NaCl(s), $NaHSO_4$(s), Na_2SO_4(s), Na_2CO_3(s), KNO_3(s), KCl(s), $KHSO_4$(s), $KHCO_3$(s), K_2CO_3(s), K_2CO_3(s), $Ca(NO_3)_2$(s), $CaCl_2$(s), $CaSO_4$(s), $CaCO_3$(s), $Mg(NO_3)_2$(s), $MgCl_2$(s), $MgSO_4$(s), and $MgCO_3$(s).

For seven out of the nine cases, the equilibrium problem consisted of x equations and x unknowns, and a unique numerical equilibrium solutions existed for all species concentrations. In two cases (1300–1630 at Riverside and Claremont), the ambient RH was below the DRH of NH_4NO_3(s) (61.8%), indicating NH_4NO_3(s) could form. As discussed in Section 4, a unique numerical solution to the size-distributed concentration of NH_4NO_3(s) does not exist when NH_4NO_3(s) is produced directly or indirectly from ammonia and nitric acid gas. Since chloride was constrained to the particle phase in all cases, unique solutions to the distribution of NH_4Cl(s) did exist in all cases. The two cases in which unique numerical solutions to the distribution of NH_4NO_3(s) were not possible are not discussed here, but all other cases are.

Fig. 1a–g compares the predicted equilibrium size-distributed ammonium and nitrate concentrations with measurements from the seven cases with unique solutions. In most size bins of every case, ammonium and nitrate predictions matched measurements reasonably. The only significant error occurred at 1300–1630 at Long Beach, where accumulation-mode nitrate was overpredicted. Some discrepancies can be seen for individual bins, such as for nitrate in the 1.04-μm bin from 0500 to 0830 at Riverside. The relative agreement between equilibrium calculations and observations, in general, suggests that, in these cases, the assumption of equilibrium may have been reasonable.

In all cases, the equilibrium model predicted calcium to be partitioned among Ca^{2+}, $CaSO_4 \cdot 2H_2O$(s) and $CaCO_3$(s). Thus, calcium was partly dissolved and partly solid. The dissolved form of calcium was made possible in part by the presence of nitrate, which led to the partial dissociation of calcium carbonate, as discussed shortly. Magnesium was always in the form of Mg^{2+}, except that in the afternoon at Long Beach, it was also present as $MgSO_4$(s). The DRH of $MgSO_4$(s) is 86.1% while that of $CaSO_4 \cdot 2H_2O$(s) is 97% (e.g., Kim and Seinfeld, 1995).

7. The effects of calcium and magnesium

It has been hypothesized that mineral aerosols containing Ca may react with and neutralize HNO_3(g) (e.g., Dentener et al., 1996; Hayami and Carmichael, 1997,1998; Tabazadeh et al., 1999). A net reaction that describes this process is

$$CaCO_3(s) + 2HNO_3(g) \rightleftharpoons Ca^{2+} + 2NO_3^- + CO_2(g) + H_2O(aq) \quad (29)$$

(Dentener et al., 1996; Tabazadeh et al., 1999). The resulting $Ca(NO_3)_2$ should normally be in the dissolved, dissociated phase since its solid phase does not easily form. An expression, analogous to Eq. (29), for magnesium is

$$MgCO_3(s) + 2HNO_3(g) \rightleftharpoons Mg^{2+} + 2NO_3^- + CO_2(g) + H_2O(aq). \quad (30)$$

The three studies discussed above were carried out for relatively clean conditions (the free troposphere, an

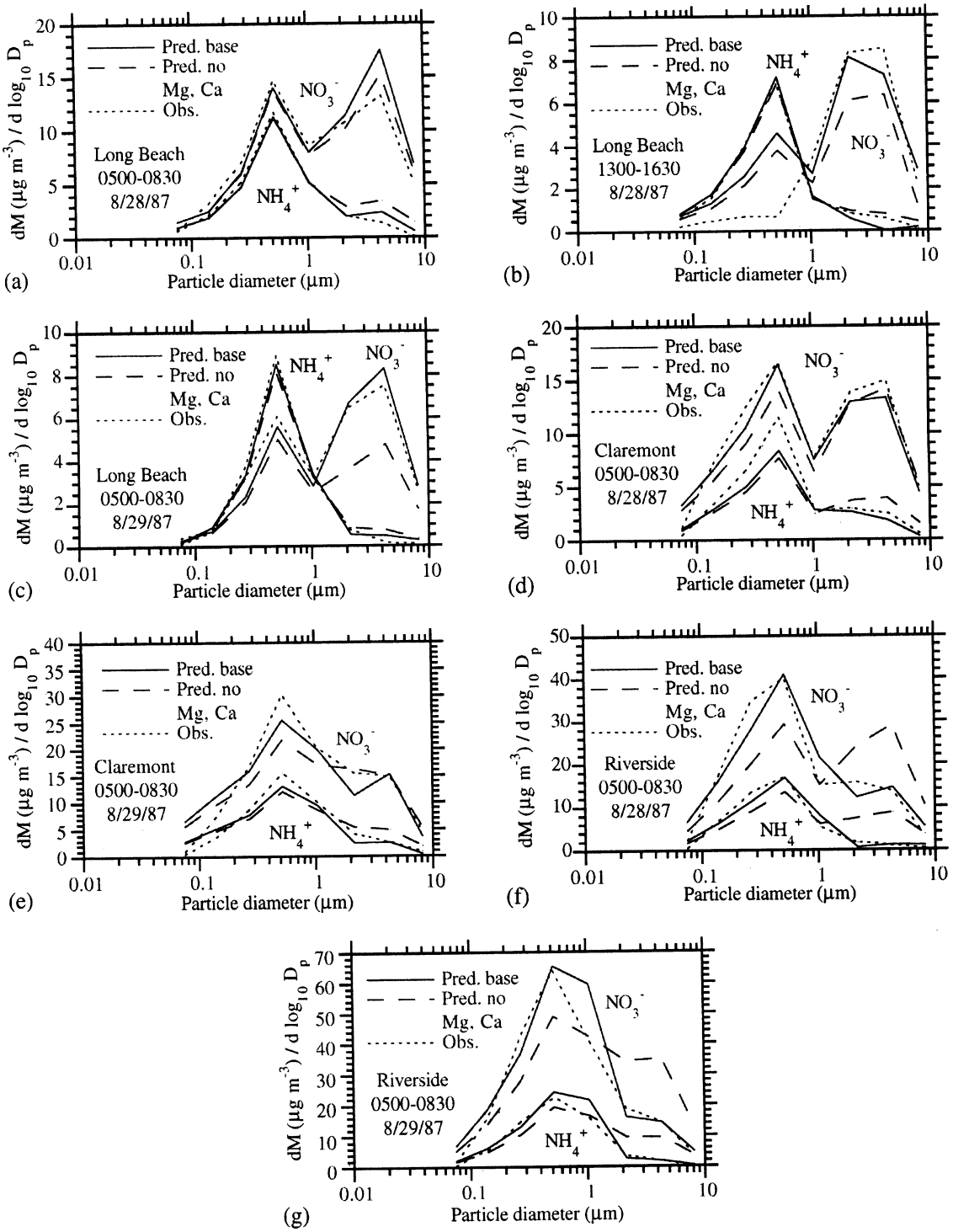

Fig. 1. Comparison of predicted with observed (John et al., 1990) size-resolved particulate nitrate and ammonium for three cases at Long Beach City College, Claremont, and Riverside. The particulate measurements ("Obs.") were resolved into 8 size bins. A baseline model simulation ("Pred. base") was initialized with observed, size distributed concentrations of NH_4^+, Na^+, Mg^{2+}, Ca^{2+}, NO_3^-, Cl^-, NO_3^-, and SO_4^{2-} and observed gas-phase concentrations of NH_3 and HNO_3 (Ca and Mg in bin 8 were initialized with values from bin 7 since no Mg or Ca data were available for bin 8). Equilibrium calculations were performed with EQUISOLV II to estimate the predicted partitioning of ammonium and nitrate between the gas phase and multiple size-bins of the aerosol phase. Chloride was constrained to the particle phase since gas-phase HCl data were unavailable. A sensitivity test was run in which Mg^{2+} and Ca^{2+} were excluded from the calculations ("Pred. no Mg, Ca"). The times are Pacific Standard Time (PST).

island offshore of South Korea, and the upper troposphere, respectively). An interesting question is whether the reaction in Eq. (29) is dominant in a more polluted location, such as Los Angeles. To examine this question, sensitivity tests were run for the cases described in the last section. For the tests, calcium and magnesium were removed from the equilibrium calculations previously performed.

Fig. 1a–g shows results from the sensitivity tests. Fig. 1a–c show that, at Long Beach, where nitrate and ammonium were much lower than at Riverside, the removal of coarse-mode calcium and magnesium reduced coarse-mode nitrate in all cases. Nitrate also decreased in the accumulation mode, but to a lesser extent than in the coarse mode in all cases. Ammonium increased in the coarse mode and decreased slightly in the accumulation mode in all cases. The reduction in coarse-mode nitrate at Long Beach upon removal of calcium and magnesium is consistent with (29) and (30). When calcium and magnesium were removed, nitrate volatalized to $HNO_3(g)$ to maintain charge balance.

The increase in coarse-mode ammonium can be explained in terms of the reaction $NH_3(g) + HNO_3(g) \rightleftharpoons NH_4^+ + NO_3^-$. The equilibrium-coefficient expression for this reaction is given in Eq. (2). The activity coefficient in Eq. (2) is a mixed activity coefficient that accounts for the binary activity coefficients of NH_4^+ in combination with all anions in solution (e.g., NO_3^-, HSO_4^-, SO_4^{2-}, Cl^-, HCO_3^-, CO_3^{2-}) and NO_3^- in combination with all cations in solution (e.g., Mg^{2+}, Ca^{2+}, Na^+, NH_4^+, H^+). At the same ionic strength, the binary activity coefficients of $Mg(NO_3)_2$ and $Ca(NO_3)_2$ are larger than that of NH_4NO_3, which replaces $Mg(NO_3)_2$ and $Ca(NO_3)_2$ as the dominant coarse-mode electrolyte in the absence of Ca and Mg. Thus, the mixed activity coefficient $\gamma^2_{NH_4^+,NO_3^-}$ is larger when Ca and Mg are present than when they are absent. For example, at 0500 on August 29, in Long Beach, the predicted $\gamma^2_{NH_4^+,NO_3^-}$ in stage 7 was 0.1455 when Ca and Mg were present but 0.0982 when they were absent. Since removing Ca and Mg reduced $\mathbf{m}_{NO_3^-}$ and $\gamma^2_{NH_4^+,NO_3^-}$ in the coarse mode at Long Beach, $\mathbf{m}_{NH_4^+}$ was required to increase to satisfy Eq. (2).

At Riverside (Fig. 1f–g), the removal of Ca and Mg from the coarse mode increased coarse-mode nitrate, which is an effect opposite to that at Long Beach and to what was expected from Eqs. (29) and (30). Removal of Ca and Mg also increased coarse-mode ammonium at Riverside more than at Long Beach. At Riverside, the concentrations of calcium, magnesium, ammonium, and nitrate were higher than at Long Beach. For example, the Ca concentration in stage 7 at 0500 on 28 August 1987 was 1.47 $\mu g\,m^{-3}$ at Riverside but only 0.26 $\mu g\,m^{-3}$ at Long Beach. Thus, when Ca and Mg were removed from particles at Riverside, the effect on $\gamma^2_{NH_4^+,NO_3^-}$ was larger than at Long Beach. Removal of Ca and Mg decreased $\gamma^2_{NH_4^+,NO_3^-}$ from 0.1156 to 0.0415 in stage 7 at Riverside at 0500 on 28 August, which is a 50% larger decrease than at Long Beach for the same time and stage. For Eq. (2) to be satisfied at Riverside, $\mathbf{m}_{NH_4^+}$ and $\mathbf{m}_{NO_3^-}$ needed to increase significantly in the coarse mode. At Long Beach, the modest change in $\gamma^2_{NH_4^+,NO_3^-}$ required $\mathbf{m}_{NH_4^+}$ to increase only slightly, allowing $m_{NO_3^-}$ to decrease.

In sum, at Long Beach, coarse-mode nitrate decreased upon removal of Ca and Mg because the charge-balance effect of Eqs. (29) and (30) dominated the activity-coefficient effect of Eq. (2). At Riverside, the activity-coefficient effect dominated the charge-balance effect, increasing nitrate concentrations upon removal of Ca and Mg. At Claremont (Fig. 1d–e) concentrations of calcium, magnesium, ammonium, and nitrate were between those at Long Beach and Riverside, and the charge-balance effect canceled the activity coefficient, resulting in little net effect of Ca and Mg on coarse-mode nitrate.

The effect of Ca and Mg on the size distribution and liquid water content are equally significant. At Long Beach, removing Ca and Mg had less effect on the accumulation mode than at Riverside. At Long Beach, the accumulation mode was controlled by sulfate, and ammonium was the primary cation to balance sulfate. When Ca and Mg were removed from the coarse mode, coarse-mode ammonium increased slightly, and coarse-mode nitrate decreased. The source of the new coarse-mode ammonium was accumulation-mode ammonium, which was transferred through the gas phase. When accumulation-mode ammonium decreased, accumulation-mode nitrate also had to decrease to maintain charge balance. Thus, removal of Ca and Mg at Long Beach reduced nitrate across the size distribution, increasing nitric acid gas, and shifting ammonium from the accumulation to the coarse mode. The reduction in particulate nitrate reduced its associated hydrated liquid water. At 0500 on 29 August, removal of Ca and Mg reduced the predicted total liquid water content from 57 to 53 $\mu g\,m^{-3}$. Most liquid water reduction was in the coarse mode.

At Riverside, accumulation-mode sulfate was less than at Long Beach and was dwarfed by accumulation-mode nitrate. When Ca and Mg were removed from the coarse mode, coarse-mode nitrate and ammonium increased at Riverside. The source of new coarse-mode nitrate and ammonium was accumulation-mode nitrate and ammonium. Material was transferred through the gas phase without much change in $HNO_3(g)$ or $NH_3(g)$. For example, at 0500 on 29 August at Riverside, about 14.6 and 3.9 $\mu g\,m^{-3}$ of nitrate and ammonium, respectively (about 22 and 19% of total particulate nitrate and ammonium, respectively), were transferred from the smallest five stages to the largest three stages when Ca and Mg were removed from the coarse mode. The corresponding changes in $HNO_3(g)$ and $NH_3(g)$ were only $+0.01$ and -1.3 $\mu g\,m^{-3}$, respectively. Because nitrate and ammonium increased in the coarse mode when Ca and Mg were removed, coarse-mode liquid water increased.

Analogously, accumulation-mode liquid water content decreased due to reduction in ammonium and nitrate. The changes in liquid water in the two modes nearly offset each other. At 0500 on 29 August at Riverside, about 18 $\mu g\ m^{-3}$ of liquid water was transferred from the accumulation mode to the coarse mode, with almost no net gain of total liquid water ($< 0.2\ \mu g\ m^{-3}$) when Ca and Mg were removed.

8. Summary

A new method of solving individual equilibrium equations was developed and incorporated into the chemical equilibrium code, EQUISOLV. EQUISOLV was also updated with thermodynamic data for potassium-, calcium-, magnesium-, and carbonate-containing species. The new version of the code is EQUISOLV II. The new solution method, the analytical equilibrium iteration (AEI) method, requires 50–100 times fewer iterations per equation to converge reactions of the form $D \rightleftharpoons 2A + B$ and $D + E \rightleftharpoons A + B$ to seven digits of accuracy than the previous method used, the Mass Flux Iteration (MFI) method. The AEI method also requires 50% fewer iterations than the MFI method to converge reactions of the form $D \rightleftharpoons 2A + B$ and $D \rightleftharpoons A + 2B$ to seven digits. Overall, EQUISOLV II, with the AEI method, converged equilibrium problems 13–48 times faster than EQUISOLV did with the MFI method in the cases tested.

Predictions of ammonium and nitrate from EQUISOLV II were compared with eight-stage Berner impactor measurements of aerosol composition from Long Beach, Claremont, and Riverside during the Southern California Air Quality Study. Comparisons were made only in high-RH cases (RH $> 62\%$), since unique numerical equilibrium solutions did not exist for lower RHs. Predictions were consistent with observations in most stages of all cases compared. A sensitivity test indicated that the removal of Ca and Mg from the coarse-mode decreased coarse-mode nitrate at Long Beach, as expected, but increased coarse-mode nitrate at Riverside, which was not expected. At Long Beach, coarse-mode nitrate decreased upon removal of Ca and Mg because a charge-balance effect dominated an activity-coefficient effect. At Riverside, the activity-coefficient effect dominated. At Claremont, the charge-balance and activity-coefficient effects nearly canceled each other, resulting in little overall effect of Ca and Mg on the size distribution.

Acknowledgements

This work was supported by grants from the Environmental Protection Agency under agreement 823186-01-0, the National Science Foundation under agreements ATM-9504481 and ATM-9614118, and the David and Lucile Packard Foundation and Hewlett-Packard company through a Stanford University Terman Fellowship.

References

Ansari, A.S., Pandis, S.N., 1999. Prediction of multicomponent inorganic aerosol behavior. Atmospheric Environment, 33, 745–748.

Bassett, M.E., Seinfeld, J.H., 1983. Atmospheric equilibrium model of sulfate and nitrate aerosol. Atmospheric Environment 17, 2237–2252.

Bassett, M.E., Seinfeld, J.H., 1984. Atmospheric equilibrium model of sulfate and nitrate aerosol. II, Particle size analysis. Atmospheric Environment 18, 1163–1170.

Binkowski, F.S., Shankar, U., 1995. The regional particulate matter model 1. Model description and preliminary results. Journal of Geophysical Research 100, 26,191–26, 209.

Bromley, L.A., 1973. Thermodynamic properties of strong electrolytes in aqueous solutions. AI.Ch.E. Journal 19, 313–320.

Clegg, S.L., Brimblecombe, P., 1988. Equilibrium partial pressures of strong acids over concentrated saline solutions – I. HNO_3. Atmospheric Environment 22, 91–100.

Clegg, S.L., Brimblecombe, P., Wexler, A.S., 1998. Thermodynamic model of the system H^+–NH_4^+–Na^+–SO_4^{2-}–NO_3^-–Cl^-–H_2O at 298.15. Journal of Physical Chemistry 102, 2155–2171.

Cohen, M.D., Flagan, R.C., Seinfeld, J.H., 1987a. Studies of concentrated electrolyte solutions using the electrodynamic balance, 1. Water activities for single-electrolyte solutions. Journal of Physical Chemistry 91, 4563–4574.

Cohen, M.D., Flagan, R.C., Seinfeld, J.H., 1987b. Studies of concentrated electrolyte solutions using the electrodynamic balance, 2. Water activities for mixed-electrolyte solutions. Journal of Physical Chemistry 91, 4575–4582.

Dentener, F.J., Carmichael, G.R., Zhang, Y., Lelieveld, J., Crutzen, P.J., 1996. Role of mineral aerosol as a reactive surface in the global troposphere. Journal of Geophysical Research 101, 22,869–22,889

Harvie, C.E., Moller, N., Weare, J.H., 1984. The prediction of mineral solubilities in natural waters: the Na–K–Mg–Ca–H–Cl–SO_4–OH–HCO_3–CO_3–CO_2–H_2O system to high ionic strengths at 25°C. Geochimica et Cosmochimica Acta 48, 723–751.

Hayami, H., Carmichael, G.R., 1997. Analysis of aerosol composition at Cheju Island, Korea, using a two-bin gas–aerosol equilibrium model. Atmospheric Environment 31, 3429–3439.

Hayami, H., Carmichael, G.R., 1998. Factors influencing the seasonal variation in particulate nitrate at Cheju Island. South Korea. Atmospheric Environment 32, 1427–1434.

Jacobson, M.Z., 1997. Numerical techniques to solve condensational and dissolutional growth equations when growth is coupled to reversible reactions. Aerosol Science and Technology 27, 491–498.

Jacobson, M.Z., 1998. Improvement of SMVGEAR II on vector and scalar machines through absolute error tolerance control. Atmospheric Environment 32, 791–796.

Jacobson, M.Z., 1999, Fundamentals of Atmospheric Modeling Cambridge University Press, New York, 656 pp.

Jacobson, M.Z., Tabazadeh, A., Turco, R.P., 1996. Simulating equilibrium within aerosols and nonequilibrium between gases and aerosols. Journal of Geophysical Research 101, 9079–9091.

John, W., Wall, S.M., Ondo, J.L., Winklmayr, W., 1990. Modes in the size distributions of atmospheric inorganic aerosol. Atmospheric Environment 24A, 2349–2359.

Kim, Y.P., Seinfeld, J.H., 1995. Atmospheric gas–aerosol equilibrium: III. Thermodynamics of crustal elements Ca^{2+}, K^{+}, and Mg^{2+}. Aerosol Science and Technology 22, 93–110.

Kim, Y.P., Seinfeld, J.H., Saxena, P., 1993a. Atmospheric gas-aerosol equilibrium, I. Thermodynamic model. Aerosol Science and Technology 19, 157–181.

Kim, Y.P., Seinfeld, J.H., Saxena, P., 1993b. Atmospheric gas-aerosol equilibrium, II. Analysis of common approximations and activity coefficient calculation methods. Aerosol Science and Technology 19, 182–198.

Kreyszig, E., 1983. Advanced Engineering Mathematics. Wiley, New York.

Meng, Z., Seinfeld, J.H., Saxena, P., Kim, Y.P., 1995. Atmospheric gas–aerosol equilibrium: IV. Thermodynamics of carbonates. Aerosol Science and Technology 23, 131–154.

Nenes, A., Pilinis, C., Pandis, S.N., 1999. ISORROPIA: a new thermodynamic model for inorganic multicomponent atmospheric aerosols. Aquatic Geochemistry, in press.

Pilinis, C., Seinfeld, J.H., 1987. Continued development of a general equilibrium model for inorganic multicomponent atmospheric aerosols. Atmospheric Environment 21, 2453–2466.

Pitzer, K.S., 1979. Ion interaction approach. In: Pytkowicz, R.M. (Ed.), Activity Coefficients in Electrolyte Solutions, Vol. I. CRC Press, Boca Raton, FL.

Pitzer, K.S., Mayorga, G., 1973. Thermodynamics of electrolytes, II, Activity and osmotic coefficients for strong electrolytes with one or both ions univalent. Journal of Physical Chemistry 77, 2300–2308.

Robinson, R.A., Stokes, R.H., 1955, Electrolyte Solutions, Second ed. Butterworths, London.

Roy, R.N., Gibbons, J.J., Wood, M.D., Williams, R.W., 1983. The first acidity constant of carbon dioxide in solutions of ammonium chloride from e.m.f. measurements at 278.15 to 318.15 K. Journal of Chemical Thermodynamics 15, 37–47.

Saxena, P., Hudischewskyj, A.B., Seigneur, C., Seinfeld, J.H., 1986. A comparative study of equilibrium approaches to the chemical characterization of secondary aerosols. Atmospheric Environment 20, 1471–1483.

Stokes, R.H., Robinson, R.A., 1966. Interactions in aqueous nonelectrolyte solutions, I. Solute–solvent equilibria. Journal of Physical Chemistry 70, 2126–2130.

Tabazadeh, A., Jacobson, M.Z., Singh, H.B., Toon, O.B., Lin, J.S., Chatfield, B., Thakur, A.N., Talbot, R.W., Dibb, J.E., 1999. Chemistry on dust in the upper troposphere. Geophysical Research Letters, 25, 4185–4188.

Tang, I.N., 1997. Thermodynamic and optical properties of mixed-salt aerosols of atmospheric importance. Journal of Geophysical Research 102, 1883–1893.

Tang, I.N., Munkelwitz, H.R., 1994. Water activities, densities, and refractive indices of aqueous sulfates and sodium nitrate droplets of atmospheric importance. Journal of Geophysical Research 99, 18,801–18,808

Wexler, A.S., Seinfeld, J.H., 1990. The distribution of ammonium salts among a size and composition dispersed aerosol. Atmospheric Environment 24A, 1231–1246.

Wexler, A.S., Seinfeld, J.H., 1991. Second-generation inorganic aerosol model. Atmospheric Environment 25A, 2731–2748. Also as a Final Report to the Coordinating Research Council Inc., Atlanta, GA 30344. Document number CPØ 28-98-2d.

Zhang, Y., Seigneur, C., Seinfeld, J.H., Jacobson, M.Z., Clegg, S.L., Binkowski, F., 1999. A comparative review of inorganic aerosol thermodynamic equilibrium modules: similarities, differences, and their likely causes. Atmospheric Environment, in review.